Quarterly Report
Massachusetts Institute of Technology
GAGE Facility GPS Data Analysis Center Coordinator
And
GAGE Facility GAMIT/GLOBK Community Support

Thomas Herring, Robert King and Mike Floyd

Period: 2016/04/01-2016/06/30

Table of Contents

Summary

Under the GAGE Facility Data Analysis subcontract, MIT has been combining results from the New Mexico Tech (NMT) and Central Washington University (CWU). In this report, we show analyses of the data processing for the period 03/13/2016 to 06/18/2016, time series velocity field analyses for the GAGE reprocessing analyses (1996-2016). Several earthquakes were investigated this quarter but none had >1 mm coseismic displacements. For this quarter the last finals results were for June 18, 2016. We added a new bad station table for sites with recently seen high position RMS values. Associated with the report are the ASCII text files that are linked into this document.

Under the GAGE Facility GAMIT/GLOBK Community Support we report on activities during this quarter.

GPS Analysis of Level 2a and 2b products

Level 2a products: Rapid products

Final and rapid level 2a products have been in general generated routinely during this quarter. The description of these products, the delivery schedule and the delivery list remain unchanged from the previous quarter and will not be reported here.

Level 2a products: Final products

The final products are generated weekly and are based on the final IGS orbits. The description of these products, the delivery schedule and the delivery list remain unchanged from the previous quarter and will not be reported here. Data volumes being transferred remains about the same. In this quarter 1914 stations were processed compared to 1913 for the previous quarter. New stations are being added and the reduction in number of stations could be due to remote site downloads and stations going off-lines

Level 2a products: 12-week, 26-week supplement products

Each week we also process the Supplemental (12-week latency) and six month supplemental (26-week latency) analyses from the ACs. The delivery schedule for these products is also unchanged.

Analysis of Final products: March 15, 2016 and June 18, 2016

Each month, we submit reports of the statistics of the PBO combined analyses and estimates of the latest velocity fields in the NAM08 reference frame based on the time series analysis of data between 1996 and month preceding the report (we need to allow 2-3 weeks for the generation of the final products). For this report, we generated the statistics using the ~3 months of results generated between March 15, 2016 and June 18, 2016. These results are summarized in Table 1 and figures 1-3.

For the three months of the final position time series generated by NMT, CWU and combination of the two (PBO), we fit linear trends and annual signals and compute the RMS scatters of the position residuals in north, east and up for each station in the analysis. Our first analysis of the distribution of these RMS scatters by analysis center and the combination. Table 1 shows the median (50%), 70% and 95% limits for the RMS scatters for PBO, NMT and CWU. The median horizontal RMS scatters are less than or equal 1.0 mm for all centers and as low as 0.74-0.75 mm for \PBO north and east components. The up RMS scatters are less than or equal 4.5 mm and as low as 3.9 mm for the NMT and PBO solutions. These statistics are similar to last quarter. Seasonal changes in atmospheric delay properties will introduce small variations in these values quarter to quarter with this quarter being slightly worse than last quarter. In the NAM08 frame realization, scale changes are not estimated. If scale changes were estimated, the up scatter would be reduced but the sum of scale change RMS and the lower height scatter would equal the values shown in Table 1. The detailed histograms of the RMS scatters are shown in Figures 1-3 for PBO, NMT and CWU.

Table 1: Statistics of the fits of 1914, 1913 and 1912 stations for PBO, NMT and CWU analyzed in the finals analysis between March 15, 2016 and June 18, 2016. Histograms of the RMS scatters are shown in Figure 1-3.

Center	North (mm)	East (mm)	Up (mm)
Median (50%)			
PBO	0.75	0.74	3.85
NMT	0.75	0.79	3.85
CWU	0.97	0.88	4.51
70%			
PBO	0.91	0.91	4.37
NMT	0.92	0.97	4.42
CWU	1.14	1.06	5.13
95%			
PBO	1.61	1.60	5.97
NMT	1.66	1.7	6.17
CWU	1.89	1.88	7.39

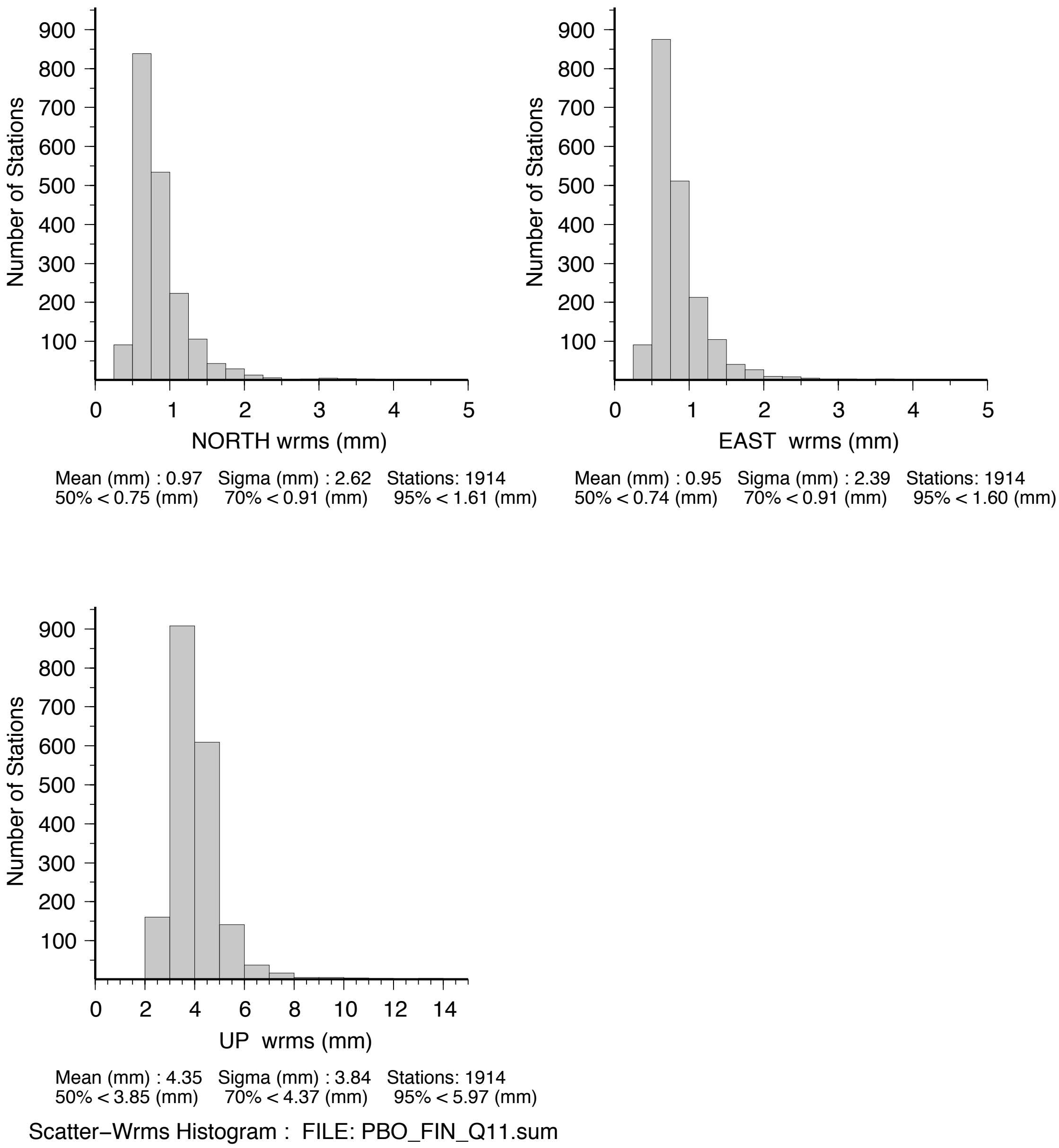

Figure 1: PBO combined solution histograms of the North, East and Up RMS scatters of the position residuals for 1914 stations analyzed between March 15, 2016 and June 18, 2016. Linear trends and annual signals were estimated from the time series.

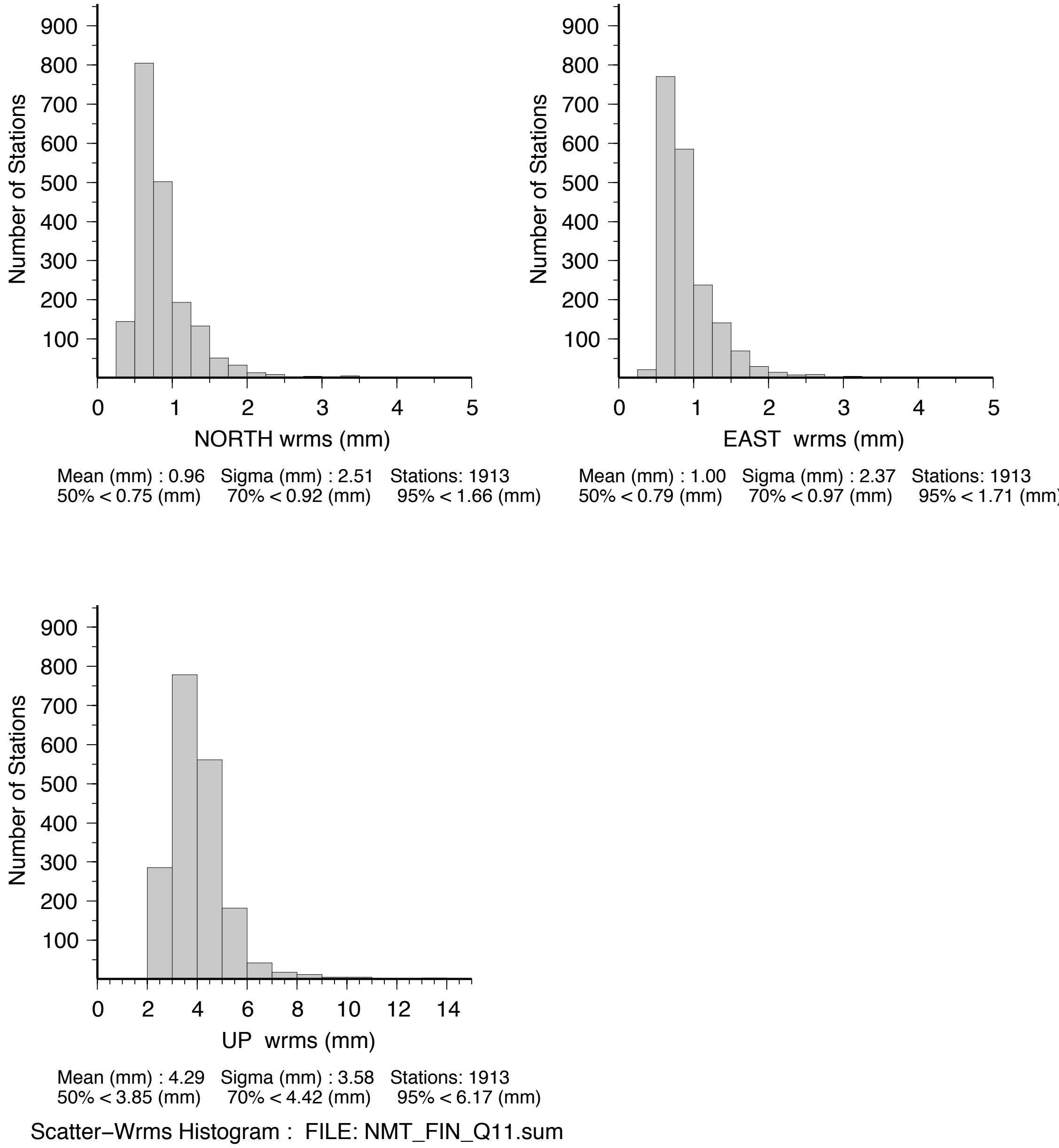

Figure 2: NMT combined solution histograms of the North, East and Up RMS scatters of the position residuals for 1913 stations analyzed between March 15, 2016 and June 18, 2016. Linear trends and annual signals were estimated from the time series.

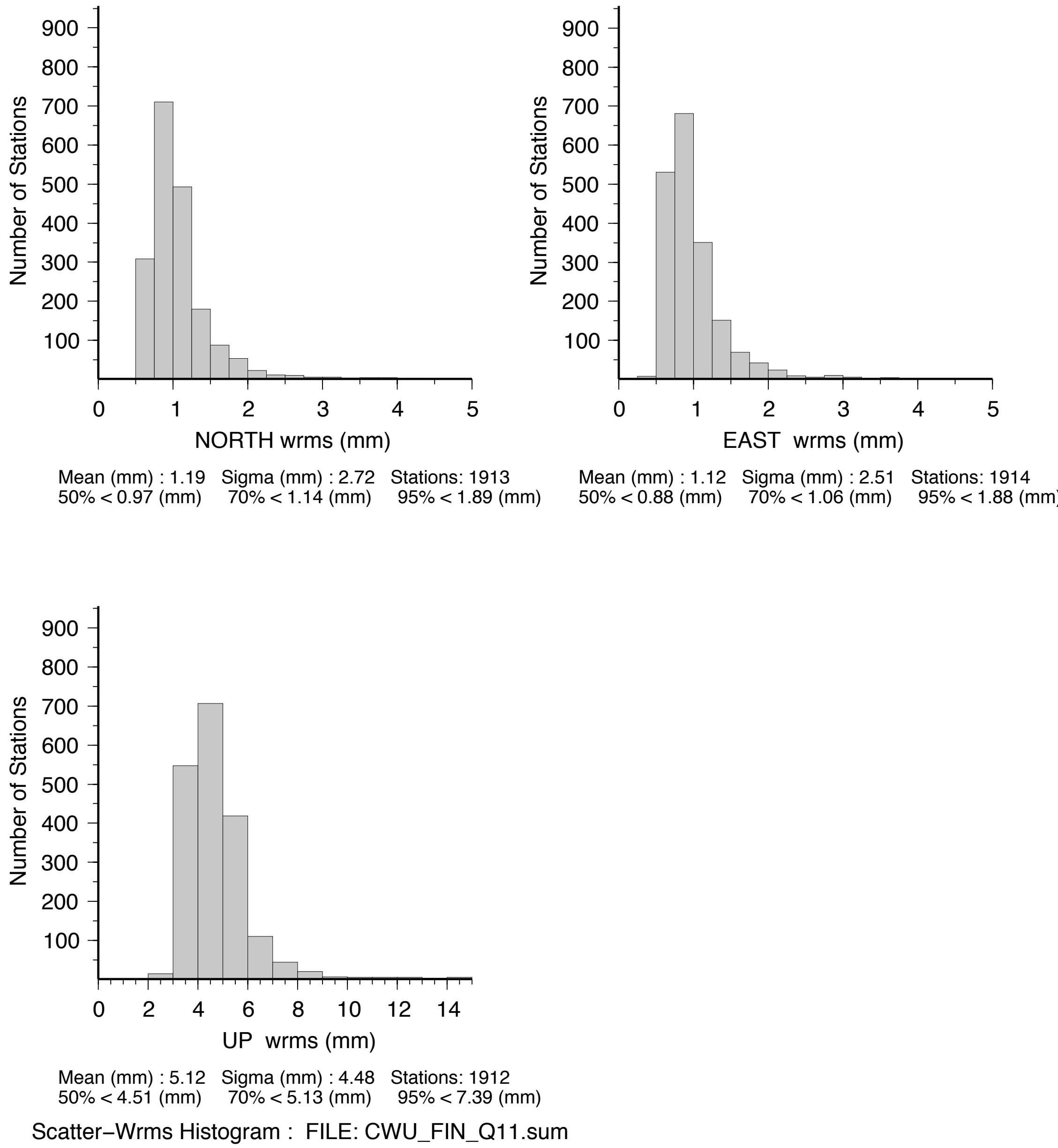

Figure 3: CWU combined solution histograms of the North, East and Up RMS scatters of the position residuals for 1912 stations analyzed between March 15, 2016 and June 18, 2016. Linear trends and annual signals were estimated from the time series.

For the PBO combined analysis, we also evaluate the RMS scatters of the position estimates by network type. The figures below are based on our monthly submissions but here we use nominally 3 months of data to evaluate the RMS scatters. In Table 2, we give the median, 70 and 95 percentile limits on the RMS scatters. The geographical distributions of the RMS scatters by network type are shown in Figures 4-9. The values plotted are given in PBO_FIN_Q11.tab. There are 1914 stations in the file. The contents of the files is of this form:

```
Tabular Position RMS scatters created from PBO_FIN_Q11.sum
ChiN/E/U are square root of chisquared degree of freedom of the fits.
Values of ChiN/E/U near unity indicate that the estimated error
bars are consistent the scatter of the position estimates

.Site     #    N (mm)  ChiN     E (mm)  ChiE   U (mm)  ChiU     Years
 1LSU    88      1.1   0.53      1.1    0.51     4.2   0.42     13.16
 1NSU    96      0.8   0.46      0.9    0.52     4.0   0.57     12.42
 1ULM    96      0.7   0.41      0.7    0.48     4.5   0.69     13.02
 7ODM    96      0.8   0.48      0.7    0.43     3.6   0.56     15.16
…
 ZBW1    96      0.8   0.39      0.9    0.53     4.8   0.69     13.04
 ZDC1    96      0.9   0.47      0.8    0.53     4.6   0.68     13.04
 ZDV1    96      0.8   0.40      0.9    0.53     4.6   0.65     13.04
 ZKC1    96      0.8   0.40      0.7    0.42     4.2   0.59     13.04
 ZLA1    96      0.8   0.41      0.8    0.43     4.3   0.58     13.04
 ZME1    96      0.9   0.49      0.7    0.43     4.2   0.57     13.27
 ZMP1    96      0.7   0.35      0.6    0.38     4.2   0.62     13.51
 ZNY1    96      0.8   0.39      0.7    0.44     4.4   0.64     13.43
 ZSE1    96      0.8   0.37      0.7    0.41     3.7   0.54     13.43
 ZTL4    96      0.8   0.41      0.7    0.39     5.0   0.66     13.62
```

Table 2: RMS scatter of the position residuals for the PBO combined solution between March 15, 2016 and June 18, 2016 divided by network type. The division of networks is based on the JAVA script unavcoMetdata.jar with network codes PBO, Nucleus, Mid-SCIGN_USGS , America_GAMA, Expanded_PBO, COCONet and Expanded_PBO

Network	North (mm)	East (mm)	Up (mm)	#Sites
Median (50%)				
PBO	0.68	0.68	3.58	849
NUCLEUS	0.67	0.67	3.46	208
USGS SCIGN	0.74	0.73	3.48	134
Expanded	0.82	0.80	4.36	596
GAMA	0.62	0.62	4.38	13
COCO Net	1.16	1.21	5.12	114
70 %				
PBO	0.83	0.82	3.93	
NUCLEUS	0.78	0.75	3.74	
USGS SCIGN	0.89	0.94	3.88	
Expanded	0.96	0.97	4.65	
GAMA	0.66	0.73	4.56	
COCO Net	1.32	1.41	5.79	
95%				
PBO	1.47	1.38	5.20	
NUCLEUS	1.37	1.19	5.46	
USGS SCIGN	1.69	1.45	5.20	
Expanded	1.58	1.67	5.87	
GAMA	0.82	0.80	4.77	
COCO Net	2.27	2.80	11.13	

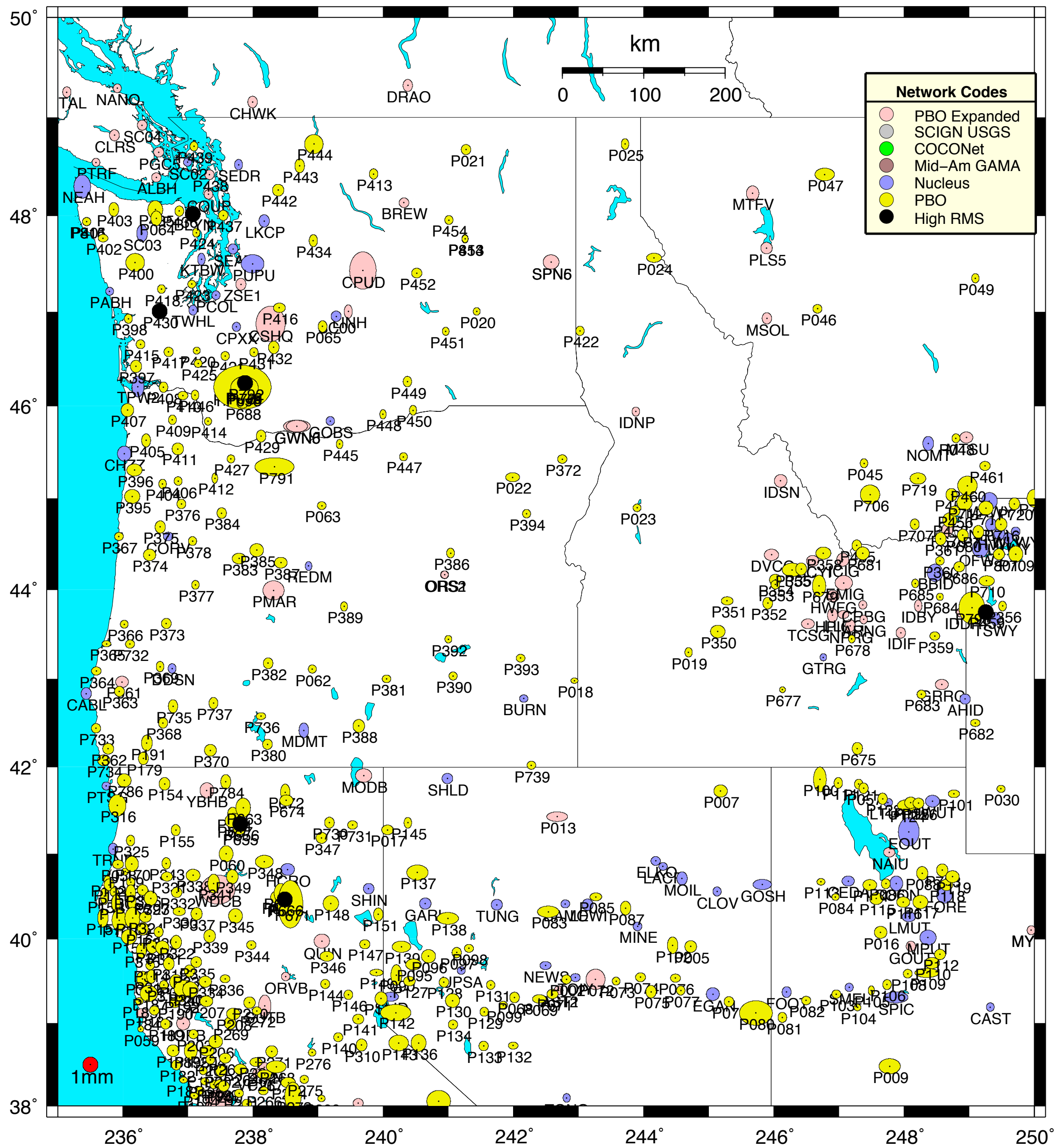

Figure 4: Distribution of the RMS scatters of horizontal position estimates from the PBO combined analysis for the Northern Western United States. The color of the ellipses that give the north and east RMS scatters denotes the network given by the legend in the figure. The small red circle shows the size of 1 mm scatters. Sites shown with black circles have combined RMS scatters in north and east greater than 5 mm or are sites that have no data during this 3-month interval.

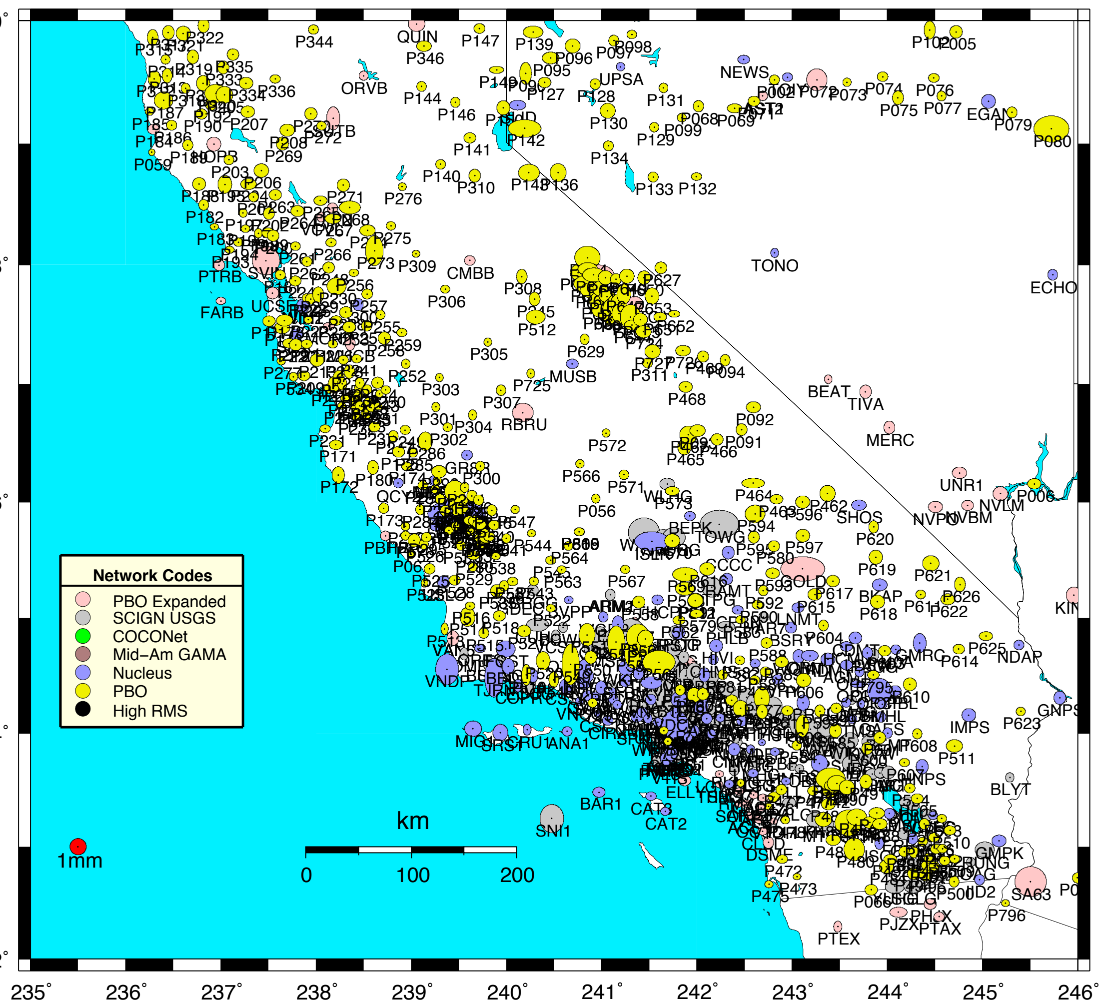

Figure 5: Same as Figure 4 except for the Southern Western United States. Black circles in the Yucca mountain region have no data during this 3-month period.

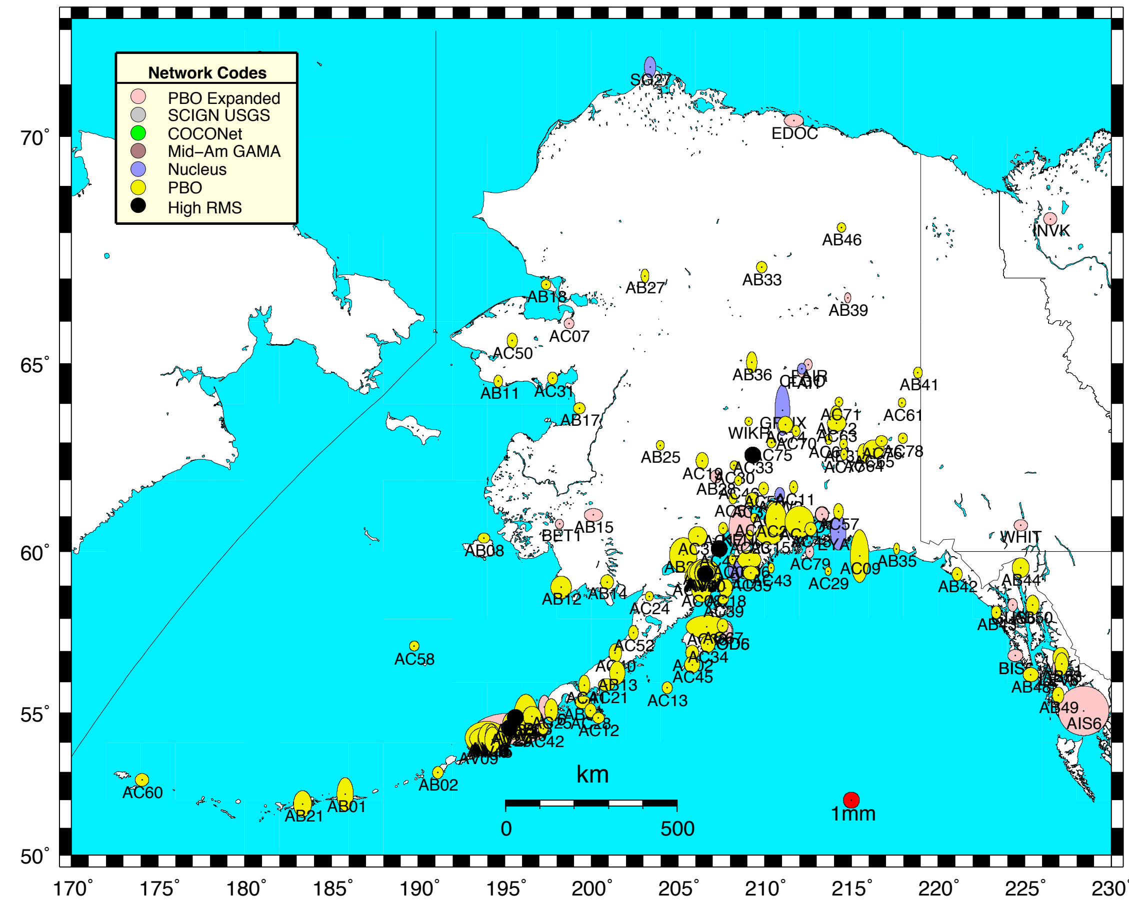

Figure 6: Same as Figure 4 except for the Alaskan region.

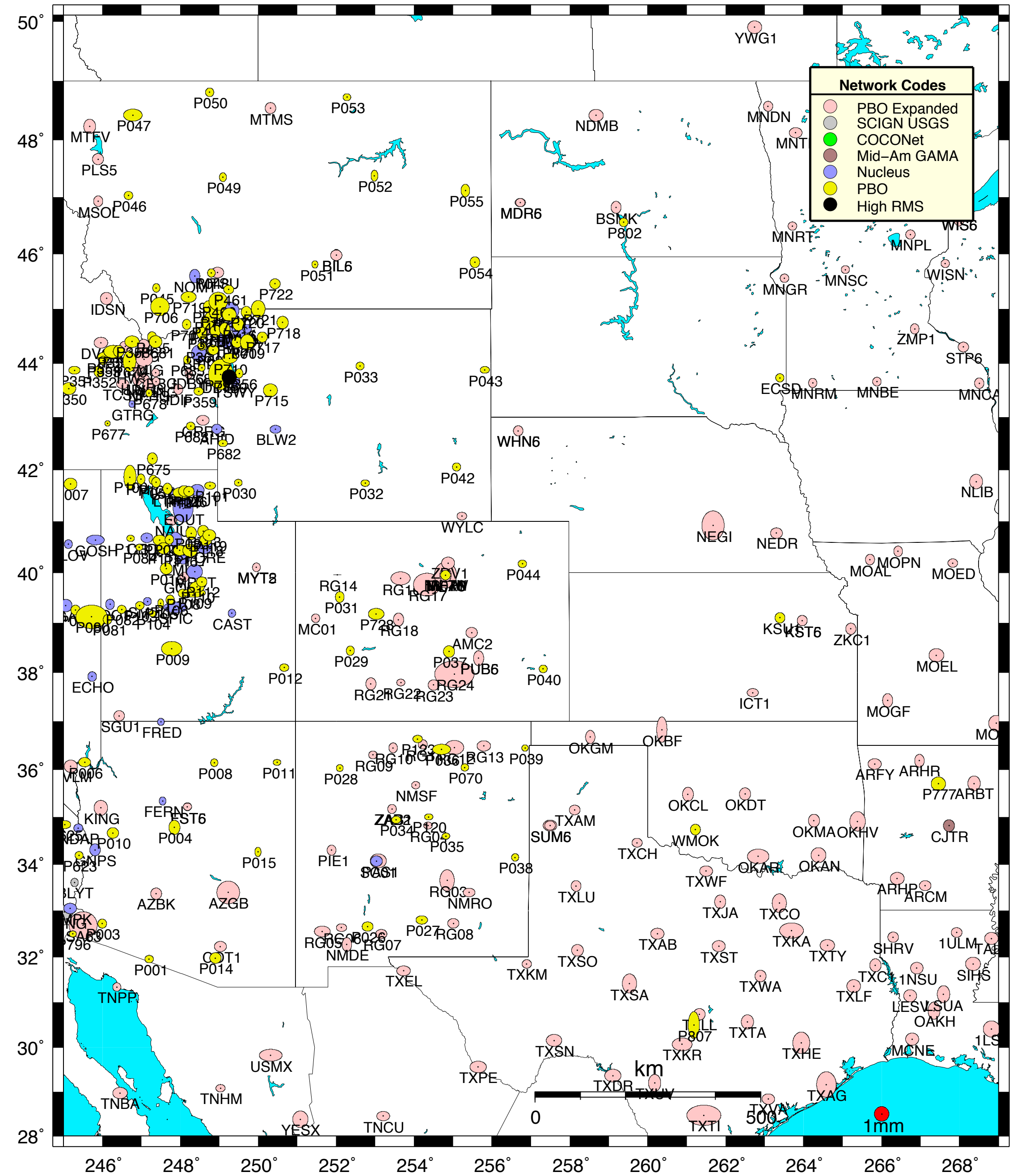

Figure 7: Same as Figure 4 except for the Central United States

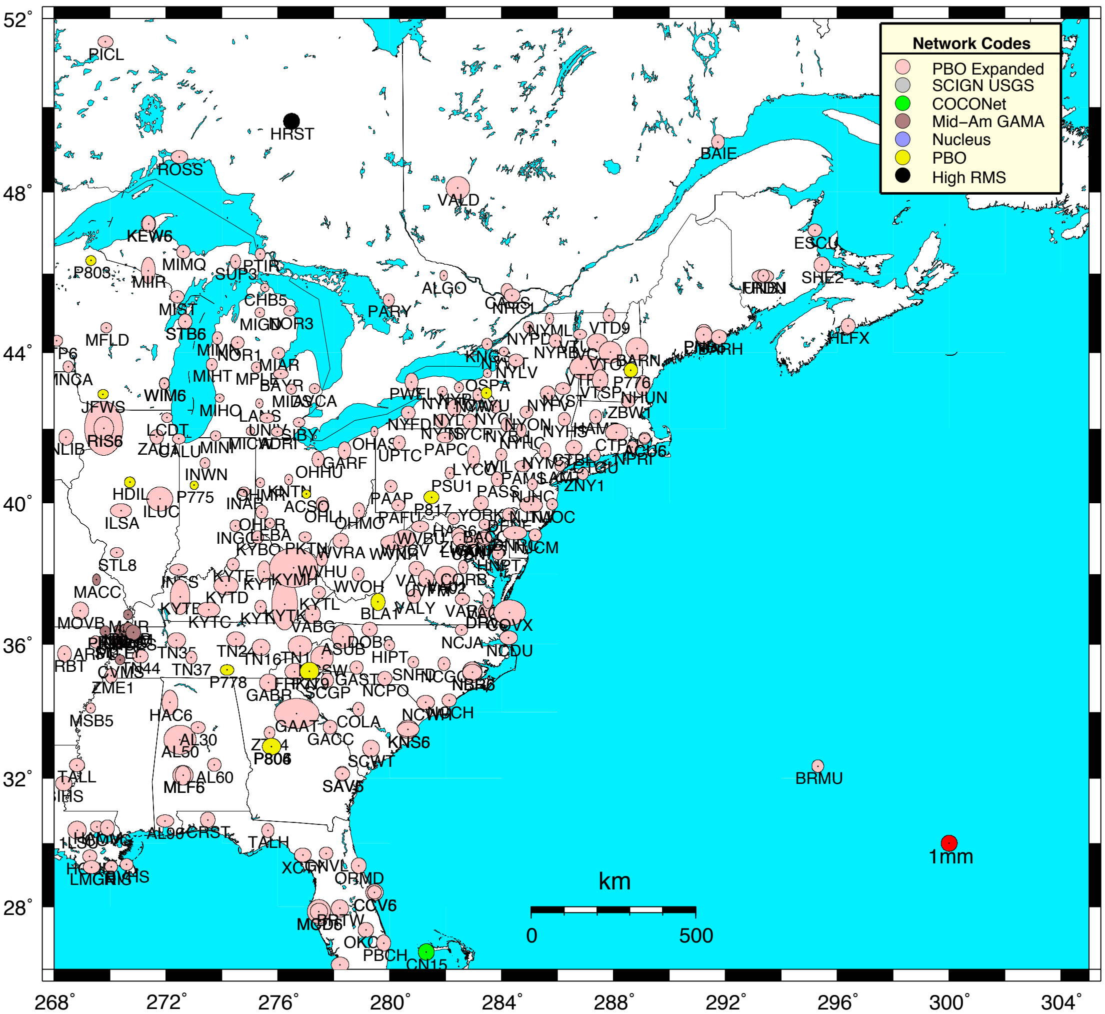

Figure 8: Same as Figure 4 except for the Eastern United States

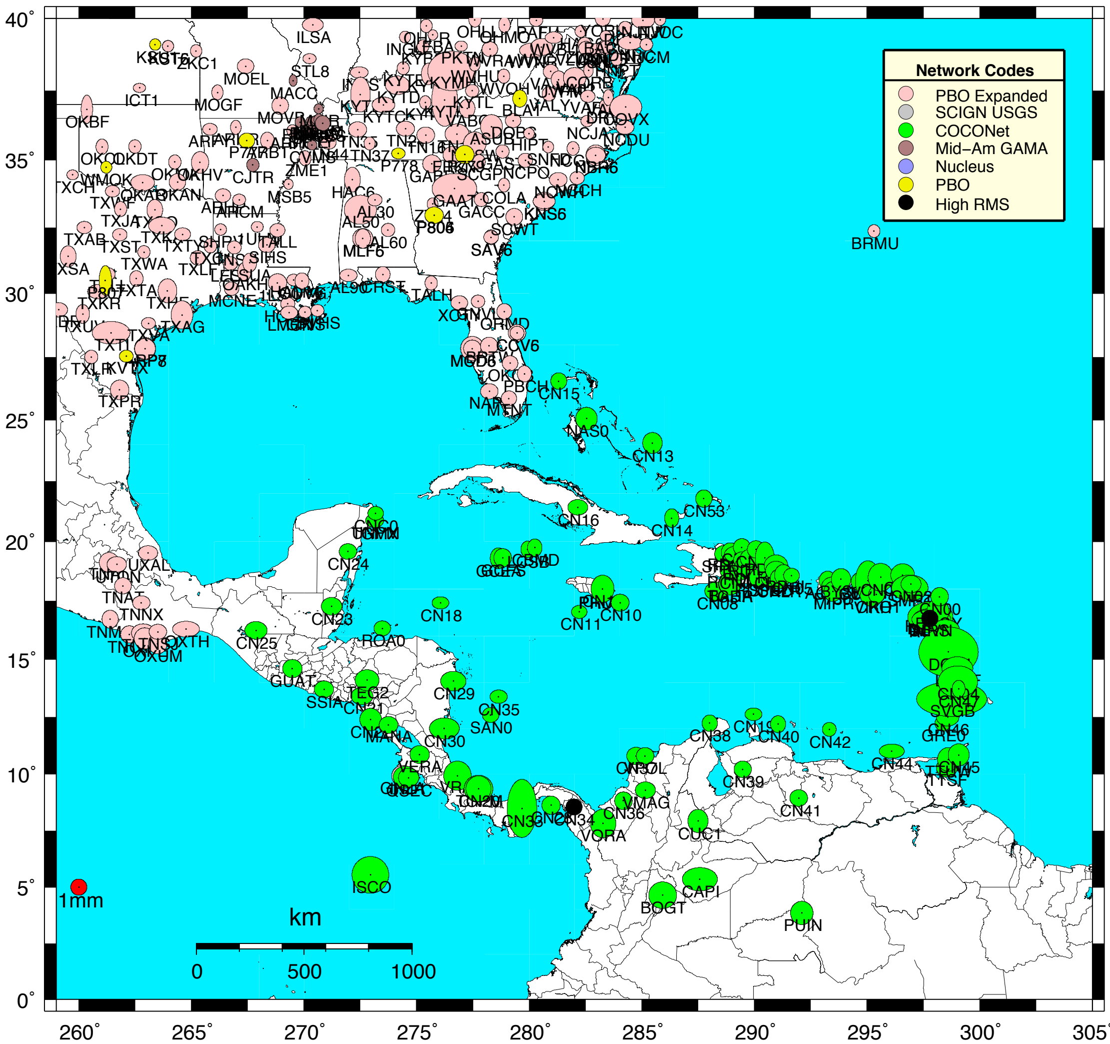

Figure 9: Same as Figure 4 except for the Caribbean region.

Analysis of large RMS stations

We add here a new analysis of high RMS scatter sites. These notes are compiled from the analysis of time series.

Table 3: Comments on time series with high RMS scatters during this quarter.

AIRS	Transient signals but 4 mm random NE RMS as well
AIS6	Bi-values residuals separated by 8 m in North and East (AIS5 does not show bifurcation but same systematics
ALPP	Skewed residuals in NE
AV20	Probably snow from 2016.1-2016.3 but very smooth
AV27	Snow most likely although systematic rather than noisy

AV35	Snow most likely although systematic rather than noisy
AV38	Skewed in the North and Height.
BLYN	Degrading since 2014.0 maybe vegetation?
BOGT	Height has large upward scatter starting ~2016. Similar behavior 2002-2005. NE look OK
CBHS	Height decrease by 30-60 mm between 04/27-05/03/2016. OK afterwards
CIT1	Jump 2012/11/07 with antenna change, poor quality and jump after 2013 11 27 switch to NetR9
CJTR	Jump on 2015/07/16 due to antenna and receiver change. Data quality better and less "annual" afterwards.
CN20	Bad results in CWU solution prior to 2015. Recent results are stable and noisy (2 mm NE 7 mm U scatter).
CN33	Station goes bad (missing data, large scatter and errorbars) starting ~11/2015.
CN34	Very systematic, seems to be degrading with time
CVMS	Bad antenna between 2013/03/18 and 2014/02/26 when changed
DAM2	5 mm jump in North 2016/03/04 for unknown reason
DOMI	Just noisy 3-5 mm NE, 15 mm U
ELTN	Noisy, NE annual and long period systematics. RMS 2.9, 1.9, 5.0 mm NEU
EOCG	Add jumps at 2016/01/06 , 2016/02/01 24 and 2016/03/06 . Added to earlier unknown jumps. 2,1.3, 6 mm scatter NEU even with jumps estimated.
EOUT	Data gets noisy and sparse starting 2015/10/06 after a gap in the time series.
EYAC	Skewed in North and Up. 2.7 mm N RMS not change recently.
GOLD	East becomes noisy starting 2014/11/20. Both CWU and NMT see the problem.
GRNX	Very skewed in N and U. No recent changes
HCES	Jump due to antenna change 2016/05/20.
HRST	Degrading since 2015. Not clear what is wrong.
ISLK	Skewed in east. RMS 2.8 mm
MFTC	Small number of outliers in N. Could be skewness.
MTGG	Little skewed in the North. 1.8 mm RMS
OLVN	Noisy and skewed in the East mostly. Systematic as well.

P429	Basically OK. Strong annual in height
P430	Looks bad after mid-2015. Could be tree. ETS signal in good data
P656	Snow? But more noise than previous years which were large and smooth,
PKRD	Just seems noisy (2mm RMS) in North. No recent change.
RDLT	A few bad data, mostly in North. Seems to happen every 4-6 months with a few days each time.
RIS5	Has strange excursions starting mid year and lasting 1-2 months. 2014 was worse than 2015.
RLAP	Noisy Mid-America sites. Bad exclusions in the past
RNCH	Strong annual in East with 3 mm RMS scatter so noisy. No recent change.
RTHS	A few recent outliers otherwise OK
RUNG	Some outliers with larger error bars. Loss of data for some reason?
SLAC	East scatter somewhat large. Some skewness can be seen
SLHG	Outliers in east (maybe skewed)
SNI1	Unknown jump 2010/02/03. East rate change and data quality degrading with time.
STLE	Mid-America site, Flagged in height but not too bad (5.3 mm).
TJRN	Skewed in the North and height. (3.1 and 5.8 mm)
TXPR	Bad patch of data with outliers in mid-2015. Seems OK again with no equipment changes
VITH	Noisy in north. Starting to have large error bars all components.
VTOX	East changes character mid 2014 and develops larger annual signal.
WASG	Noisy heights in mid-2015. Still noisy 9.5 mm.

GLOBK Apriori coordinate file and earthquake files

As part of the quarterly analysis we run complete analysis of the time series files and generate position, velocity and other parameter estimates from these time series. These files can be directly used in the GLOBK analysis files sent with the GAGE analysis documentation. These links point to the current earthquake and discontinuity files used in the GAGE ACC analyses: All_PBO_eqs.eq All_PBO_ants.eq All_PBO_unkn.eq. The GLOBK apriori coordinate file All_PBO_nam08.apr is the current estimates based on data analysis in this quarterly report. Starting in Q06, we added a GLOBK apriori

coordinate file based on the latest SNIPS PBO velocity file that are generated monthly. The SNIPS file updates the coordinates and velocities of stations that have changed in some significant fashion since the generation of the primary apriori coordinate file. The current file is All_PBO_nam08_snips.apr. Both of these apriori files are read with the –PER option in GLOBK (i.e., no periodic terms are applied). In these files, comments have a non-blank character in the first column and text after a ! in lines is treated as a comment. The apriori file contains Cartesian XYZ positions and velocities in meters with the epoch of the position in decimal years (day of year divided by days in the specific year). The comments contain the standard deviations of the estimates and are not specifically used in GLOBK (yet). The GEOD lines give geodetic coordinates and not directly used (information only). The EXTENDED lines give the extended parts of the model parameters. Specifically, OFFSETS are NEU position and velocity offsets at the times of discontinuities. The velocity changes are all zero in the PBO analyses. The Type in the comment at the end of line indicates the type of offset. If a name is given then this is an antenna or unknown origin offset. For earthquakes, EQ is the type and two characters after is the code for the earthquake. If postseismic motion is model, then LOG or EXP EXTENDED lines will appear. The time constant of the function is given after the date (days) and the amplitudes in meters in NEU frame is given after that. The comment contains the standard deviations in mm. PERIODIC terms give the period (days) after the date and then cosine and sine terms in NEU. The periodic terms are not used in the standard GLOBK analyses. The comment contains the standard deviations. The GLOBK apriori coordinate file contains annual periodic terms but these are not used in the daily reference frame realization.
When interpreting the offsets in the apriori file, it is important to note that these are obtained for a simultaneous analysis of all data from a site. If the residuals to the fit are systematic, the offsets often will not be the same as an offset computed from analysis of shot spans of data on either side of the offset. We are considering adding such an analysis type in the future.

Snapshot velocity field analysis from the reprocessed PBO analysis.

In our monthly reports, we generate "snapshot" velocity fields in the NAM08 reference frame based on the time series analysis of all data processed to that time. We have now started to distribute the snapshot fields (SNAPS) and the significant updates to the standard PBO velocity file (SNIPS file) in standard PBO velocity field format. These files are distributed in the monthly reports. For this quarterly report, we generate these velocity estimates for the reprocessed results and the current GAGE analyses that are in the NAM08 reference frame. There are 2184 stations in the combined PBO solution, which is 28 more stations than last quarter. The statistics of the fits to results are shown in Table 4. In this analysis, offsets are estimated for antenna changes and earthquakes. Annual signals are estimated and for some earthquakes, logarithmic post-seismic signals are also estimated. The full tables of RMS fits along with the duration of the data used are given in the following linked files: pbo_nam08_160618.tab, nmt_nam08_160618.tab and cwu_nam08_1603618.tab. The velocity estimates are shown by region and network type in Figures 10-16. The color scheme used is the same as Figures 4-9. The snapshot velocity field files are linked as: pbo_nam08_160618.snpvel, nmt_nam08_160618.snpvel and cwu_nam08_160618.snpvel.

Table 4: Statistics of the fits of 2183, 2182 and 2176 stations analyzed by PBO, NMT and CWU in the reprocessed analysis for data collected between Jan 1, 1996 and June 18, 2016. (LTUT is not included in the statistics and thus the 2183 versus 2184 in the text).

Center	North (mm)	East (mm)	Up (mm)
Median (50%)			
PBO	1.13	1.17	5.31
NMT	1.13	1.22	5.73
CWU	1.34	1.31	5.98
70%			
PBO	1.45	1.48	5.99
NMT	1.46	1.56	6.48
CWU	1.66	1.63	6.79
95%			
PBO	3.18	3.07	8.88
NMT	3.17	3.11	9.05
CWU	3.43	3.30	10.14

Different tolerances are used for maximum standard deviation in each of the figures so that regions with small velocity vectors can be displayed at large scales without the plots being dominated by large error bar points. The standard deviations of the velocity estimated are computed using the GLOBK First-order-Gauss-Markov Extrapolation (FOGMEX) model that aims to account for temporal correlations in the time series residuals. This algorithm is also called the "Realistic Sigma" model.

A direct comparison of the NMT and CWU solutions shows the weighted root-mean-square (WRMS) difference between the two velocity fields is 0.08 mm/yr horizontal and 0.74 mm/yr vertical from differences of all stations with in 0.5 meters of each other (the difference in number of values arises from groups of sites within). The χ^2/f of the difference is $(1.16)^2$ for the horizontal and $(1.98)^2$ vertical components. These comparisons are summarized in Table 5. As noted in previous reports, adding small minimum sigmas, computed such that χ^2/f is near unity changes the statistic slightly (Table 5). With the FOGMEX correlated noise model used to compute the velocity sigmas, the comparison statistics are close but still 18-94% optimistic over expectations. The 10-worst stations are JNPR, LST1, MCD1, MCD5, MYT2, P282, P713, P801, SAV1 and SAV5. This is the same list as the previous quarter.

Table 5: Statistics of the differences between the CWU and NMT velocity solutions with no transformation between them. In these comparisons stations with the same names and within 0.5 meters of each other are included and the total number of comparisons is larger than the number of stations. The PBO, NMT and CWU solutions themselves have 2178, 2177 and 2170 stations. WRMS is weighted-root-mean-scatter and NRMS is sqrt(χ^2/f)

where f is the number of comparisons. Larger numbers of stations appear below because stations with 500 meters of each other are included in the counts.

Solution	#	NE WRMS (mm/yr)	U WRMS (mm/yr)	NE NRMS	U NRMS
All	2192	0.08	0.74	1.16	1.98
Edited -10 worst	2175	0.07	0.72	1.05	1.94
Less than median (0.14 0.45 mm/yr)	1229	0.06	0.65	1.12	2.08
Added minimum sigma NE 0.05 U 0.50 mm/yr					
All	2187	0.12	1.03	0.95	1.14
Edited -10 worst	2170	0.10	0.98	0.85	1.09
Less than median (0.15 0.0.67 mm/yr)	1262	0.07	0.77	0.74	0.94

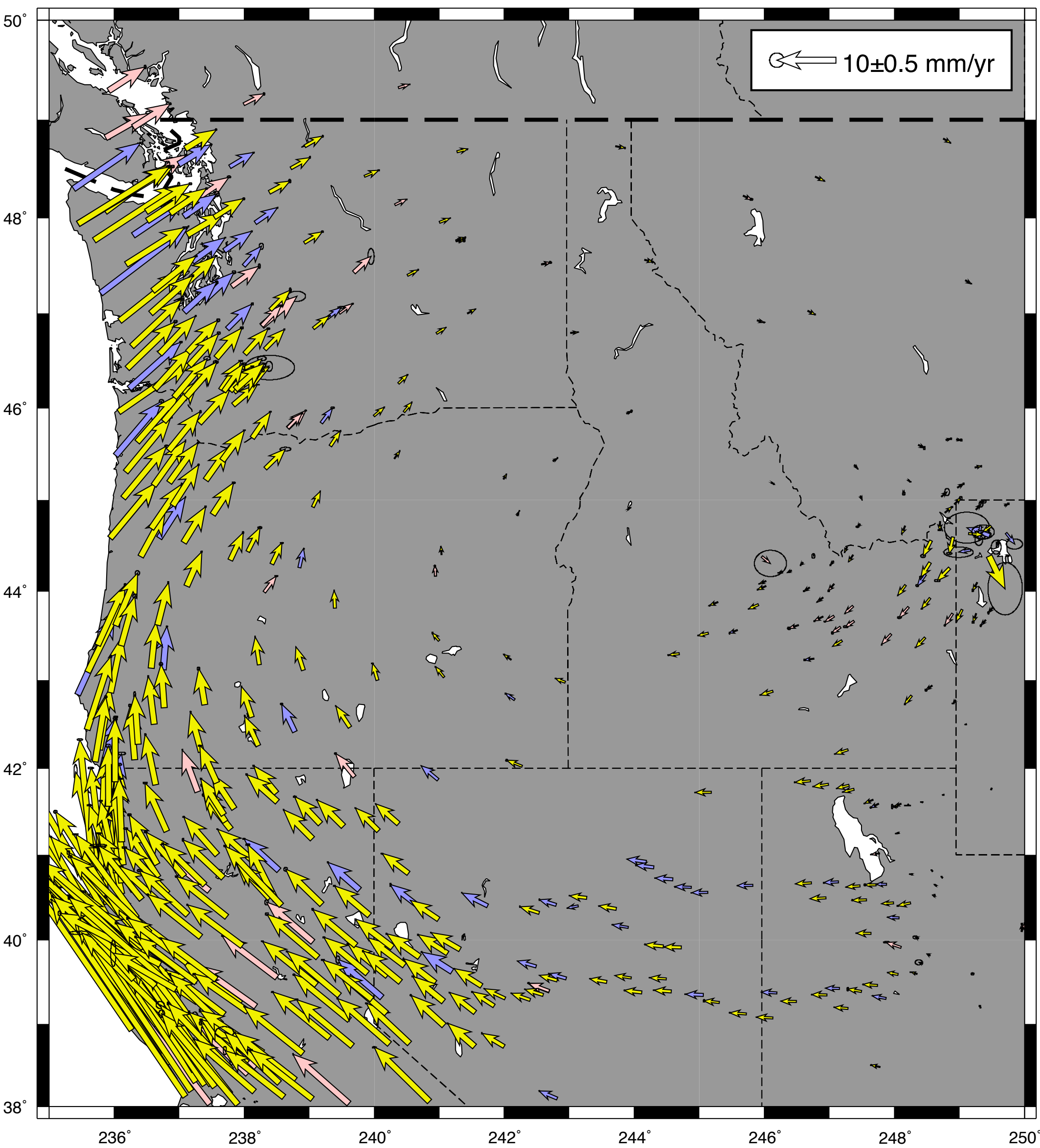

Figure 10: Velocity field estimates from the combined PBO solutions generated using time series analysis and the FOGMEX error model. 95% confidence interval error ellipses are shown. The color scheme of the vectors matches the network type legend in Figure 4. Only velocities with horizontal standard deviations less than 2 mm/yr are shown (this value is reduced from previous reports due the improved velocity sigmas).

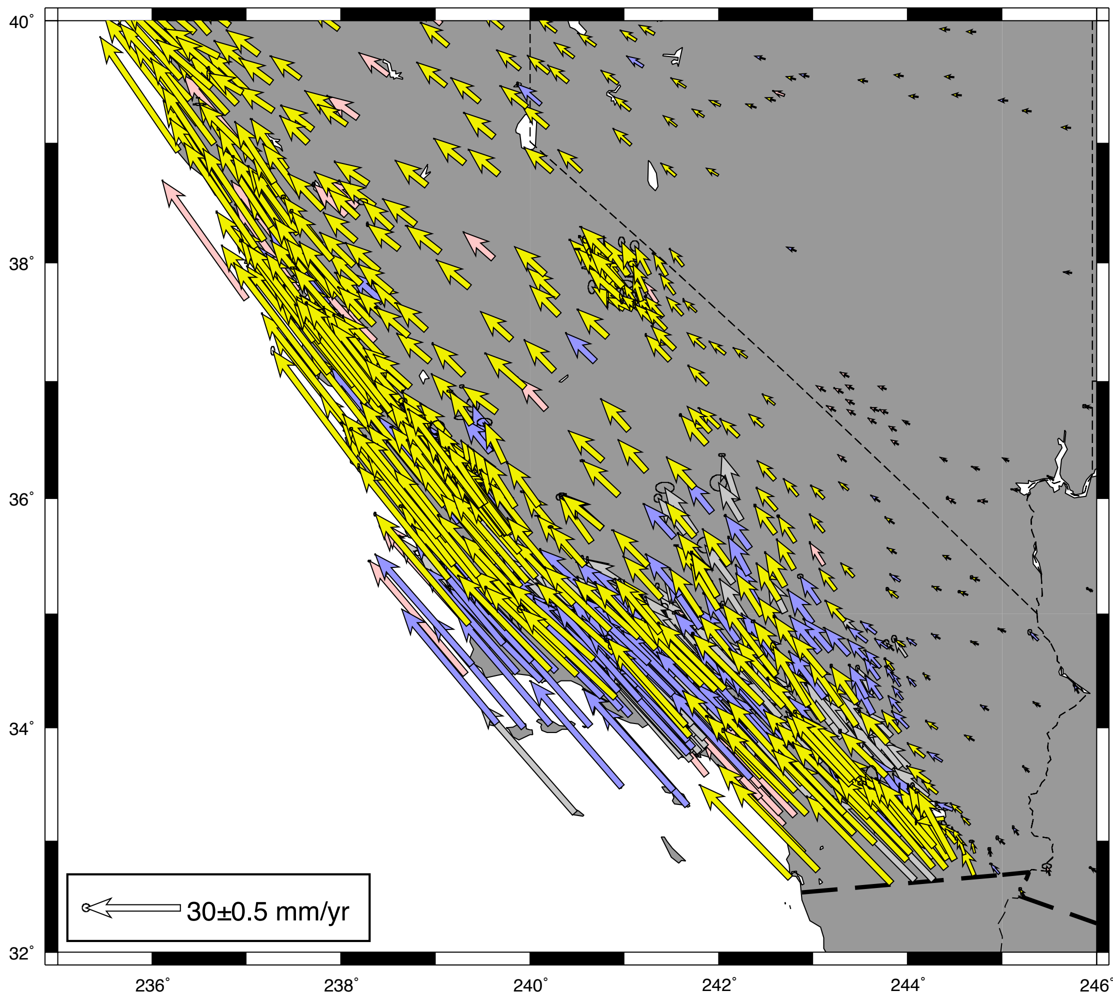

Figure 11: Same as Figure 10 except for South Western United States. Only velocities with horizontal standard deviations less than 2 mm/yr are shown.

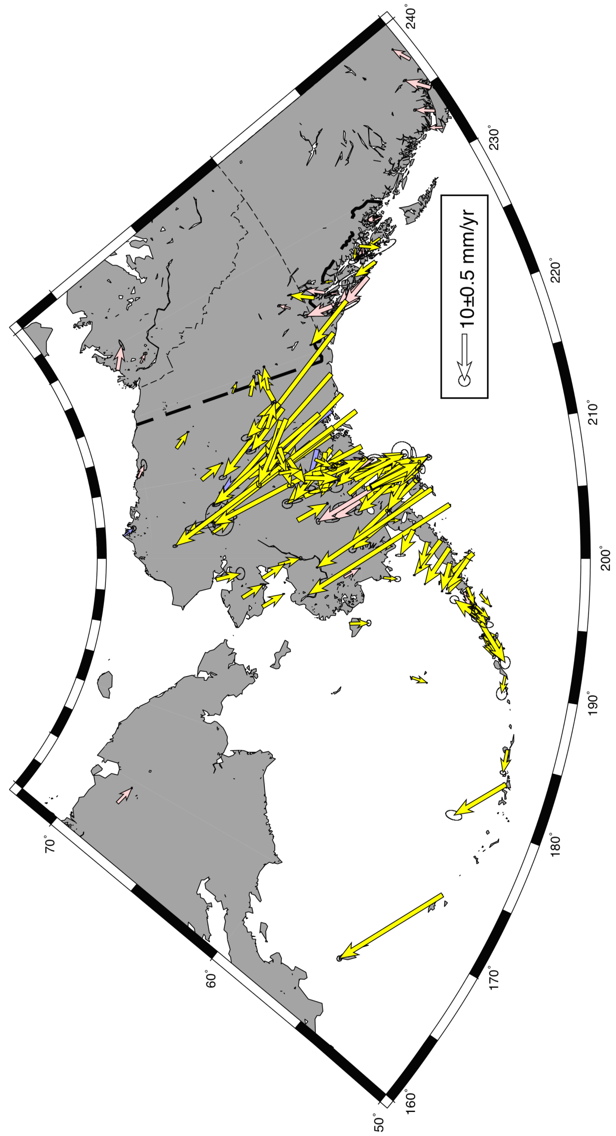

Figure 12: Same as Figure 10 except for Alaska. Only velocities with horizontal standard deviations less than 5 mm/yr are shown

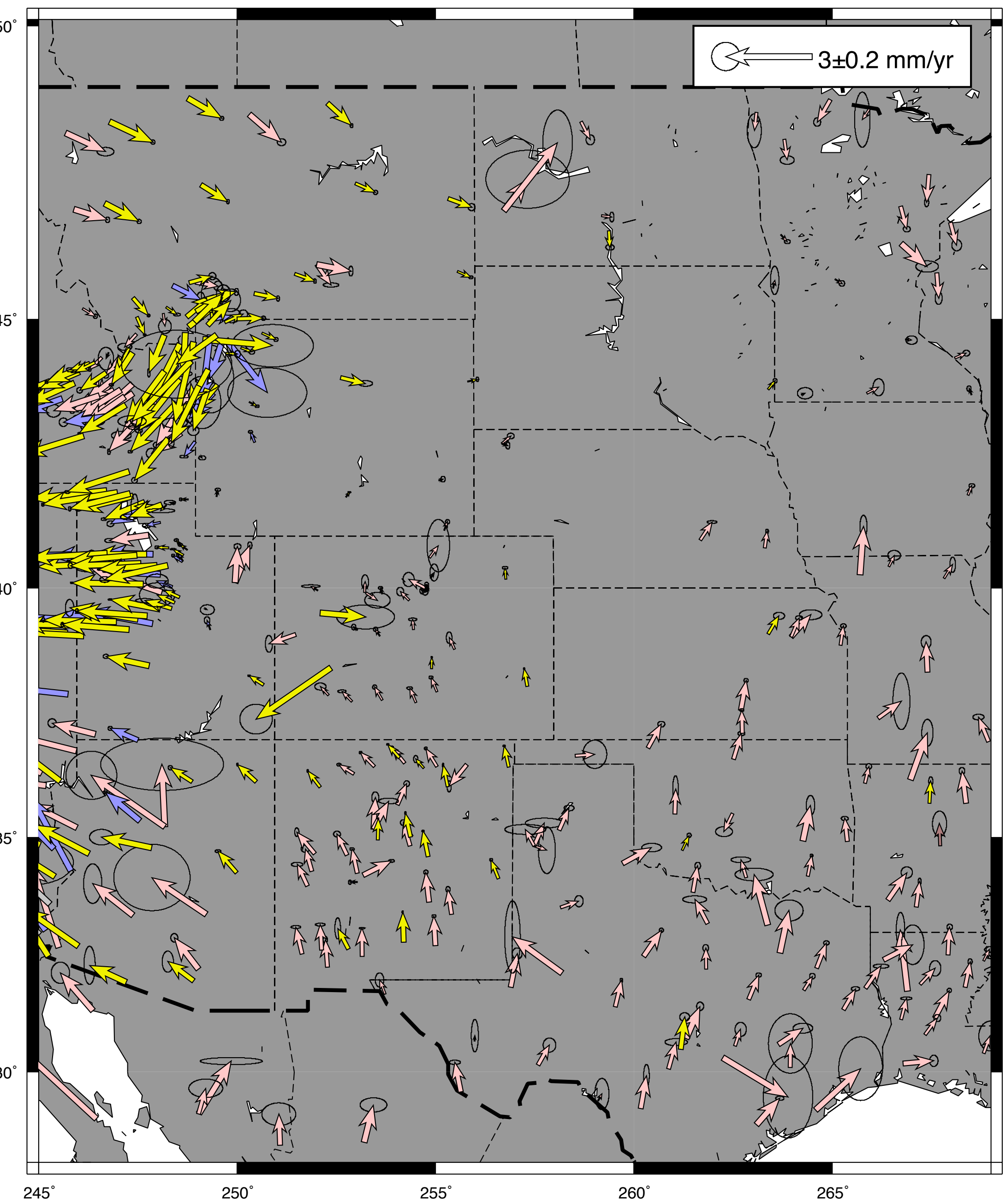

Figure 13: Same as Figure 10 except for Central United States. Only velocities with horizontal standard deviations less than 1 mm/yr are shown.

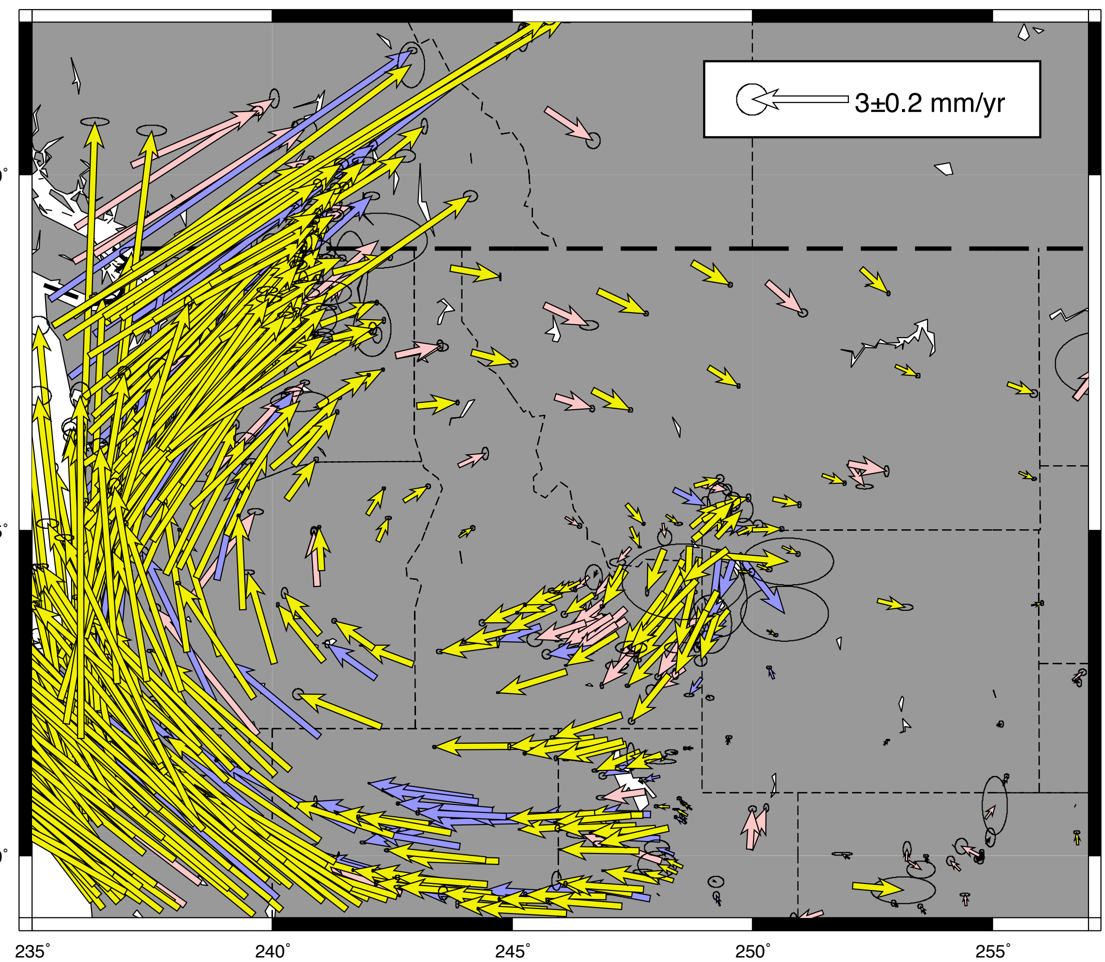

Figure 14: Same as Figure 10 except for Western Central United States. Only velocities with horizontal standard deviations less than 1 mm/yr are shown. Anomalous vectors at longitude 250^{o} are in the Yellowstone National Park and most likely are showing volcanic processes.

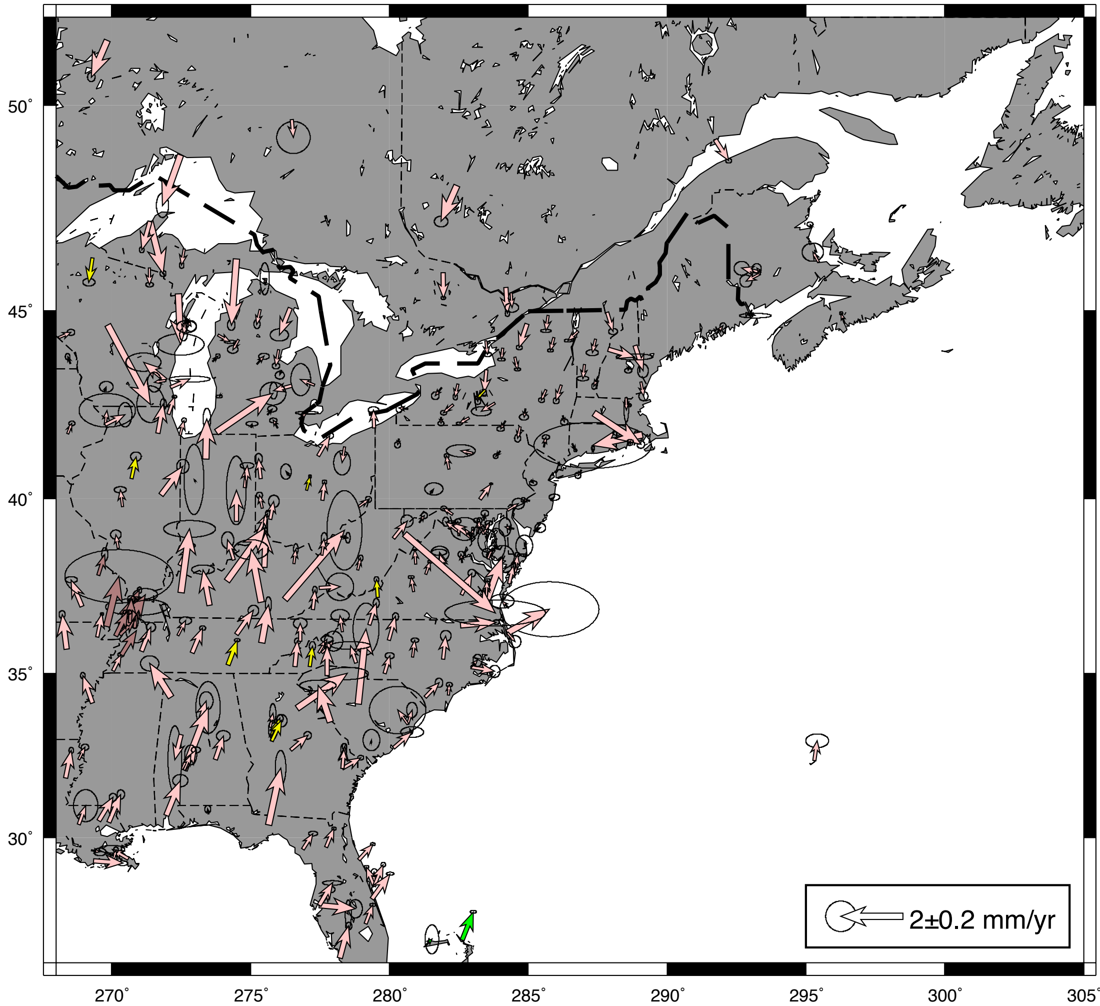

Figure 15: Same as Figure 10 except for the Eastern United States. Only velocities with horizontal standard deviations less than 2 mm/yr are shown. The systematic velocity of sites in the Northeast and central US show deviations for current GIA models in the horizontal velocities. The vertical motions match quite well but geodetic vertical motions are already included in the development of the models. Horizontal GIA motions will affect the North America Euler pole from ITRF2008.

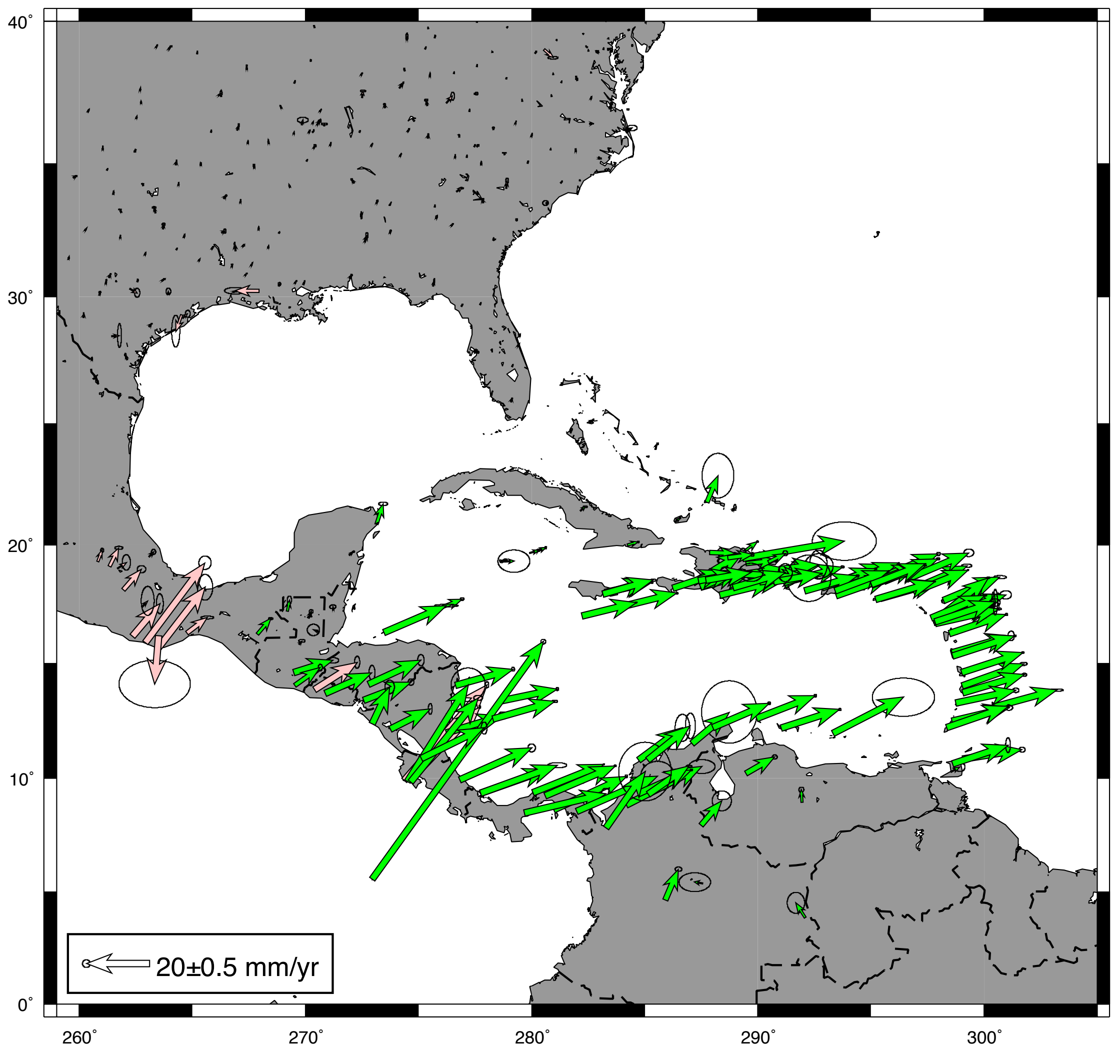

Figure 16: Same as Figure 10 except for the Caribbean region. Only velocities with horizontal standard deviations less than 5 mm/yr are shown.

Earthquake Analyses: 2016/03/01-2016/05/31.

We use the NEIC catalog to search for earthquakes that could cause coseismic offsets at the sites analyzed by the GAGE analysis centers. We examined the following earthquakes. In these output, each earthquake that might have generated coseismic displacements is numbered and the “SEQ Earthquake # n” starts the block of information about the earthquake. The EQ MM lines, give station name, distance from hypocenter (km), maximum distance that could cause coseismic offsets > 1 mm, and the “CoS” (coseismic offset) value is the possible offset in the mm. The eq_def lines give the event number, latitude, longitude, radius of influence, and depth of event followed by the date and time of the event. If an event is found to be significant, the event number is modified to reflect the total number of events so far included in the PBO analyses. Large events are often given a two-character code to reflect their location (e.g., PA is Parkfield).

In March/April 2016 we investigated the following events.

```
* EQDEFS for 2016 03 14 to 2016 04 17 Generated Sun Apr 17 02:58:01 EDT 2016
* Proximity based on Week_All.Pos file
* ---------------------------------
* SEQ Earthquake # 1
* EQ 640 P203_GPS       7.44       9.10 CoS        0.0 mm
* EQ_DEF M3.8 9km NW of The Geysers
 eq_def 01   38.8263 -122.8495      9.1 8 2016 04 08 12 59    0.000
 eq_rename 01
 eq_coseis 01  0.001 0.001 0.001      0.000      0.000      0.000
```

Only one earthquake was found this month and it generated no discernible offset. The 7.8Mw earthquake "27km SSE of Muisne, Ecuador" did not affect any GAGE stations. Catalog entry for this earthquake:
2016-04-16T23:58:37.280Z,0.3715,-79.9398,19.16,7.8,mww,,41,2.139,1,us,us20005j32,2016-04-17T03:27:47.181Z,"27km SSE of Muisne, Ecuador",earthquake,6.2,3.4,,,reviewed,us,us .

In April/May 2016, the following events were investigated

```
* EQDEFS for 2016 04 16 to 2016 05 15 Generated Mon May 16 15:32:39 EDT 2016
* Proximity based on Week_All.Pos file
* ---------------------------------
* SEQ Earthquake # 1
* EQ 466 AC18_GPS       5.86      14.70 CoS       16.8 mm
* EQ_DEF M4.9 94km SSW of Homer
 eq_def 01   58.8989 -152.3383     14.7 8 2016 04 29 08 18    0.009
 eq_rename 01
 eq_coseis 01  0.001 0.001 0.001      0.009      0.009      0.009
* ---------------------------------
* SEQ Earthquake # 2
* EQ 647 CN00_GPS      10.74      14.70 CoS        5.0 mm
* EQ_DEF M4.9 13km E of Codrington
 eq_def 02   17.6396  -61.6904     14.7 8 2016 05 08 13 49    0.009
 eq_rename 02
 eq_coseis 02  0.001 0.001 0.001      0.009      0.009      0.009
```

Neither of these earthquakes generated measurable co-seismic offsets at the sites.

In May/June 2016, the following events were investigated but none show co-seismic offsets.

```
* EQDEFS for 2016 05 14 to 2016 06 15 Generated Tue Jun 14 15:30:20 EDT 2016
* Proximity based on Week_All.Pos file
* ---------------------------------
* SEQ Earthquake # 1
* EQ 160 MIDA_GPS       7.90       8.70 CoS        0.0 mm
* EQ 160 MNMC_GPS       8.18       8.70 CoS        0.0 mm
* EQ 160 P292_GPS       6.21       8.70 CoS        0.0 mm
* EQ 160 P297_GPS       2.51       8.70 CoS        0.0 mm
* EQ 160 P789_GPS       5.38       8.70 CoS        0.0 mm
* EQ 160 P790_GPS       4.48       8.70 CoS        0.0 mm
* EQ 160 PKDB_GPS       3.02       8.70 CoS        0.0 mm
* EQ 160 POMM_GPS       6.85       8.70 CoS        0.0 mm
* EQ 160 RNCH_GPS       7.65       8.70 CoS        0.0 mm
* EQ_DEF M3.5 24km SW of Coalinga
 eq_def 01   35.9687 -120.5262      8.7 8 2016 05 17 22 59    0.000
 eq_rename 01
 eq_coseis 01  0.001 0.001 0.001      0.000      0.000      0.000
```

```
* ----------------------------------
* SEQ Earthquake # 2
* EQ 599 CN27_GPS       3.20       9.80 CoS        6.2 mm
* EQ_DEF M4.1 7km NW of Cabrera
 eq_def 02   19.6866  -69.9637      9.8 8 2016 06 05 00 34    0.001
 eq_rename 02
 eq_coseis 02  0.001 0.001 0.001      0.001      0.001      0.001
* ----------------------------------
* SEQ Earthquake # 3
* EQ 681 P707_GPS       6.16       8.90 CoS        0.0 mm
* EQ_DEF M3.7 52km W of West Yellowstone
 eq_def 03   44.7328 -111.7632      8.9 8 2016 06 09 03 32    0.000
 eq_rename 03
 eq_coseis 03  0.001 0.001 0.001      0.000      0.000      0.000
* ----------------------------------
* SEQ Earthquake # 4
* EQ 697 CN22_GPS      50.99      53.90 CoS        4.6 mm
* EQ_DEF M6.1 17km E of Puerto Morazan
 eq_def 04   12.8410  -87.0131     53.9 8 2016 06 10 03 26    0.187
 eq_rename 04
 eq_coseis 04  0.001 0.001 0.001      0.187      0.187      0.187
* ----------------------------------
* SEQ Earthquake # 5
* EQ 705 P484_GPS      17.81      18.30 CoS        3.4 mm
* EQ 705 P490_GPS      10.34      18.30 CoS       10.2 mm
* EQ 705 P741_GPS      16.31      18.30 CoS        4.1 mm
* EQ 705 P742_GPS      16.59      18.30 CoS        4.0 mm
* EQ_DEF M5.2 20km NNW of Borrego Springs
 eq_def 05   33.4315 -116.4427     18.3 8 2016 06 10 08 05    0.017
 eq_rename 05
 eq_coseis 05  0.001 0.001 0.001      0.017      0.017      0.017
* ----------------------------------
* SEQ Earthquake # 6
* EQ 753 P707_GPS       6.06      10.70 CoS        3.5 mm
* EQ_DEF M4.3 52km W of West Yellowstone
 eq_def 06   44.7302 -111.7637     10.7 8 2016 06 13 12 15    0.002
 eq_rename 06
 eq_coseis 06  0.001 0.001 0.001      0.002      0.002      0.002
* ----------------------------------
* SEQ Earthquake # 7
* EQ 770 P707_GPS       6.00       9.50 CoS        1.8 mm
* EQ_DEF M4.0 52km W of West Yellowstone
 eq_def 07   44.7325 -111.7652      9.5 8 2016 06 14 14 36    0.001
 eq_rename 07
 eq_coseis 07  0.001 0.001 0.001      0.001      0.001      0.001
```

None of these earthquakes generated measurable co-seismic offsets at the sites including the M5.2 20km NNW of Borrego Springs on June 10. This event was reported in the news.

Antenna Change Offsets: 2016/03/01-2016/05/31

The follow antenna changes were investigated and reported on in the MIT ACC monthly reports.

```
Station      Date           From           To
 KNTN  2016  3 29 13 30 TRM55971.00   TRM59900.00
 OXPE  2016  3  1 19  6 Radome NONE   SCIT
 OXUM  2016  3 10 23  3 TRM41249.00   TRM57971.00
 P059  2016  3 15 18 15 TRM29659.00   TRM59800.80
 PASS  2016  3  2 15 11 TRM41249.00   TRM57971.00
```

```
 TEG2  2016  3  4 15  9 TRM55971.00   TRM41249.00

 COON  2016  4 21  0  0 TRM59800.80   TRM29659.00
 P227  2016  4 22  0  0 TRM29659.00   TRM59800.80
 P228  2016  4 21 19 27 TRM29659.00   TRM59800.80
 P229  2016  4 22  0  0 TRM29659.00   TRM59800.80
 P230  2016  4 22  0  0 TRM29659.00   TRM59800.80
 P513  2016  4 27  0  0 TRM29659.00   TRM59800.80
 RDON  2016  4 28  0  0 TRM55971.00   TRM59800.00

 HCES  2016  5 20  0  0 ASH700936D_M  TRM57971.00
 INEG  2016  5 20 18  0 TRM29659.00   LEIAR10
 OXTH  2016  5 16 17 36 TRM41249.00   TRM57971.00
 P406  2016  5 13  0  0 TRM29659.00   TRM59800.80
 P427  2016  5 28  0  0 TRM29659.00   TRM59800.80
 P807  2016  5  8  0  0 TRM29659.00   TRM59800.80
```

Analysis
KNTN: WLS dNEU 4.34 ± 1.23, 1.39 ± 2.05, -1.39 ± 14.02 mm,
KF dNEU 4.24 ± 0.39, 1.31 ± 0.34, 0.38 ± 1.56 mm .
The north offset is clear in the data.
OXPE: WLS dNEU -4.28 ± 3.58, -1.83 ± 2.62, -11.30 ± 2.45 mm,
KF dNEU -3.39 ± 2.30, -2.33 ± 1.96, -11.36 ± 3.02 mm
Large gap in data (since 2015.5) makes offset difficult to judge.
OXUM: WLS dNEU -1.93 ± 1.21, -1.06 ± 1.06, 0.86 ± 2.83 mm,
KF dNEU -1.76 ± 1.44, 0.03 ± 1.33, 3.23 ± 3.78 mm
Similar to above with a large gap in the data.
P059: WLS dNEU 0.87 ± 1.55, -0.95 ± 0.53, -1.90 ± 4.12 mm,
KF dNEU 0.08 ± 0.28, -1.45 ± 0.24, -3.07 ± 0.88 mm
Annual removed when estimate made. There is a one-month gap in the time series making assessment of this break more difficult.
PASS: WLS dNEU -2.69 ± 0.57, 1.28 ± 0.94, -6.73 ± 2.26 mm,
KF dNEU -2.19 ± 0.31, 1.59 ± 0.28, -6.69 ± 1.01 mm
About a two-week gap in the data before antenna change.
TEG2: WLS dNEU 1.57 ± 13.11, -0.23 ± 3.59, 6.12 ± 10.42 mm,
KF dNEU -0.85 ± 1.10 , -0.33 ± 0.91, 6.31 ± 3.46 mm
Large gap data (3 months) and poor quality of data after antenna change with only 4 rapid estimates available make this jump difficult to interpret at the time of the monthly. With new data now available, the offset estimates are from the Kalman Filter 0.40 ± 0.66, 1.65 ± 0.46 and 34.69 ±1.33 mm. The height offset looks significant.

COON WLS dNEU -0.89 ± 1.81, 3.53 ± 1.81, -4.18 ± 10.93 mm,
KF dNEU -0.89 ± 0.42, 3.93 ± 0.37, -10.56 ± 1.47 mm
Data has gaps before the antenna change and it not clear how significant these offsets are.
P227 WLS dNEU 1.40 ± 0.97, 3.13 ± 1.09, -1.91 ± 6.27 mm,
KF dNEU 0.99 ± 0.31, 1.72 ± 0.29, 0.82 ± 1.19 mm
Offsets here are small.
P228 WLS dNEU 0.30 ± 0.75, -2.39 ± 1.29, -4.73 ± 7.07 mm,
KF dNEU 0.35 ± 0.33, -4.02 ± 0.32, -0.62 ± 1.31 mm
The east offset here can be clearly seen in the time series.

P229 WLS dNEU -0.30 ± 3.35, 4.77 ± 1.72, -6.69 ± 5.88 mm,
KF dNEU -2.67 ± 0.31, 3.08 ± 0.27, -6.12 ± 1.01 mm
The offsets in North and east estimated by the Kalman filter can be seen in the data.
P230 WLS dNEU 0.78 ± 3.01, 3.75 ± 5.45, 0.11 ± 20.12 mm,
KF dNEU -0.10 ± 0.38, 3.05 ± 0.37, -0.91 ± 1.45 mm
The east offset is visible in the time series and there are 3-outlier values (few mm) that are seen in both the CWU and NMT solutions.
P513 WLS dNEU -1.34 ± 1.56, -0.35 ± 1.03, -2.07 ± 7.88 mm,
KF dNEU -1.28 ± 0.31, -1.21 ± 0.29, -3.99 ± 1.12 mm
There is a 23-day (and poor quality results prior to then) that make the estimates of these offsets not particularly robust.
RDON WLS dNEU 1.93 ± 1.48, -3.54 ± 2.03, -3.73 ± 5.60 mm,
KF dNEU 1.63 ± 0.62, -3.25 ± 0.74, -4.18 ± 2.56 mm
Large gap in the data (from 2015-10-04 to 2016-04-20) make these estimates not very robust at the time. Additional data confirm the horizontal offsets but the Kalman Filter height offset is now 6.60 ± 1.55 mm.

HCES: WLS dNEU 10.42 ± 3.61, -39.27 ± 13.95, -15.84 ± 11.64 mm,
KF dNEU 11.76 ± 0.51, -41.02 ± 0.62, -11.69 ± 1.90 mm
The east jump is very clear in the data.
INEG: WLS dNEU 0.58 ± 6.21, 7.59 ± 2.68, -15.59 ± 17.79 mm,
KF dNEU -2.41 ± 0.50, 6.50 ± 0.43, -6.72 ± 1.90 mm
The jump looks pretty clear in the time series but there is long period curvature to the time series that can corrupt the offset estimates.
OXTH: WLS dNEU -4.78 ± 1.09, 6.71 ± 3.12, 29.00 ± 5.63 mm,
KF dNEU -4.35 ± 0.54, 7.13 ± 0.82, 26.78 ± 2.50 mm
Data is noisy and sparse so these are not very robust estimates of the offsets at the time. Adding recent data to the estimates reduces the height offset to 14.52 ± 1.55 mm.
P406: WLS dNEU 4.01 ± 1.92, -0.05 ± 2.38, 1.07 ± 6.58 mm,
KF dNEU 3.99 ± 0.32, -0.06 ± 0.26, 1.15 ± 1.04 mm
The north offset is clear in the time series but estimate can be affected by non-secular episodic transients before the antenna change. These transients are ETS like with a period of ~700 days. Offset estimated at 2016/02/20 with data around this time deleted to account for likely ETS event.
P427: WLS dNEU -0.98 ± 1.37, -3.01 ± 2.81, 3.27 ± 8.17 mm,
KF dNEU -0.97 ± 0.46, -2.98 ± 0.37, 3.33 ± 1.50 mm
Similar situation to P406 (same region) but east shows the ETS events most clearly.
P807: WLS dNEU -2.66 ± 1.30, 0.93 ± 0.54, -1.86 ± 7.97 mm,
KF dNEU -2.96 ± 0.33, 0.91 ± 0.31, 0.92 ± 1.44 mm
The north residual show a fair amount of skewness and so this offset is not so clear but there does seem to a north offset.

MIT issued advisories

While looking at the effects of the antenna changes at the P227-P229 sites we noticed that the M 5.6 at 37.430 -121.770 on 2007 10 31 3 4 (7km NNE of East foothills, CA; near San Jose) probably has a long term post-seismic transient associated with it. This transient is mostly in the North direction and is strongest at P227 P228 and P253. Other sites in the area P218, P226 and P254 seem to have strong hydrology signals that make seeing the transient difficult. At P228, modeling the transient as 10-day log term changes the velocity estimates by 0.64 ± 0.18 mm.yr in the North and the RMS scatter of position residuals changes from 1.23 mm to 0.87 mm in North. To account for the transient we have added a log term for this earthquake (EQ12).

Comparison on different monument types

The GAGE analysis includes stations that use many different types of monuments. The stations installed as PBO stations were mostly deep-drilled braced and shallow-drilled braced monuments. These types of monuments were also used at a number stations from other networks that are included in the GAGE analysis. There are also a variety of other types of monuments used and for some stations the type of monument has not been included in the station metadata. The large number of stations and long data spans of the results presented here allow us to derive some basic statistical information about the position time series associated with different types of monuments. Previous studies have also examined the character of position time series associated with different monument types [e.g., *Beavan,* 2005; *Williams et al.,* 2004] and have concluded based on smaller datasets than processed here that deep-drilled braced monuments are more stable than other types of monuments. Our study supports that conclusion although much more detailed studies are possible. In Table 6, we present basic statistics of the position time series of stations with different monument types as recorded the UNAVCO data archive. Not all stations processed by GAGE are in the data archive. The table gives the WRMS scatter of the position residuals in north (N), east (E) and up (U) after fitting to our standard parameterization (see Section 3) to the time series. The table also includes the statistics of the estimates of the random walk process noise values for the horizontal coordinate. The latter statistic is used to characterize the longer period systematic trends in the data. The table gives the median and 95% quantile ranges of the statistics.

Caution should be used in interpreting the values in the tables because there are many contributions to the noise in the position time series other than monument stability. There are geographic dependencies to the noise in the position time series reflecting the effects of levels of vegetation and tropospheric water vapor variations. Station behavior will also depend on the material into which the monument is installed (e.g., sediments versus bedrock) and the detailed geology of each station is difficult to obtain. Nevertheless, Table 6 shows that deep-drilled braced followed by shallow-drilled braced monuments have the smallest WRMS scatter and HRW values suggesting that these monuments are more stable than other types. UNAVCO also collects data specifically aimed at comparing the relative motions between nearby monuments of different types (station separations of less than a few meters). The analysis of these data will be published elsewhere but the time series for these stations appear in the standard products. The monument comparison sites are P591/P811/P812, P565/P809/P810, P804/P805/P806, P453/P813/P814 and P401/P815/P816. Differential motion between the stations at each site can be seen but these relative motions are often small compared to longer period systematics in the time series again indicating that the simple interpretation of Table 6 does not convey the full complexity of monument stability versus other sources of noise in position time series.

Table 6: Statistics of stations by monument type.
The WRMS scatter values are computed from the position residuals after removing a linear trend, discontinuities, annual signals and, for some stations, post-seismic logarithmic functions. The HRW values are estimates of the random walk process noise value in the horizontal position estimates. The Miscellaneous category include various types of monuments including stations where the monument type is unknown.

Monument type	# of stations	Median N WRMS (mm)	Median E WRMS (mm)	Median U WRMS (mm)	Median HRW (mm^2/yr)
Deep-drilled braced	694	0.93	0.97	4.87	0.107
Shallow-drilled braced	550	1.11	1.19	5.22	0.146
Building roof/wall	135	1.38	1.52	6.15	0.424
Pillar	103	1.50	1.49	5.98	0.254
Miscellaneous	258	1.29	1.34	5.83	0.362
		95% WRMS N (mm)	95% WMRS E (mm)	95% WRMS U (mm)	95% HRW (mm^2/yr)
Deep-drilled braced	694	2.18	2.39	6.94	3.274
Shallow-drilled braced	550	3.77	3.37	9.74	7.331
Building roof/wall	135	3.09	3.82	10.43	17.798
Pillar	103	5.04	3.86	15.22	10.109

Miscellaneous	258	4.63	3.94	10.30	21.349

Script updates

No major changes have been to the scripts.

GAMIT/GLOBK Community Support

During this quarter we made only minor changes to GAMIT to clean up reporting features and add new receivers and antennas. We have begun work on the coding of a yaw model for Beidou, to be followed by a model for Galileo. A primary task for the next quarter will be coding ambiguity resolution for Glonass FDMA observations, the last major hurdle before releasing a version of GAMIT/GLOBK that will handle RINEX 3 and two-frequency observations for GPS, Glonass, Beidou, and Galileo, the GNSS constellations capable of high-precision geodetic measurements.

There were no UNAVCO-sponsored data-analysis workshops during this period, but we continue to spend 5-10 hours per week in email support of users. During the quarter we issued 32 royalty-free licenses to educational and research institutions.

References

Beavan, J. (2005), Noise properties of continuous GPS data from concrete pillar geodetic monuments in New Zealand and comparison with data from U.S. deep drilled braced monuments, *J. Geophys. Res., 110*, B08410, doi:10.1029/2005JB003642.

Williams, S. D. P., Y. Bock, P. Fang, P. Jamason, R. M. Nikolaidis, L. Prawirodirdjo, M. Miller, and D. J. Johnson (2004), Error analysis of continuous GPS position time series, *J. Geophys. Res., 109*, B03412, doi:10.1029/2003JB002741.